

**Transcriptional Basis for Exercise Limitation in Male eNOS Knockout Mice with  
Age-Related Heart Failure and the Fetal Phenotype**

Caroline Ojaimi<sup>1</sup>, Wei Li<sup>1</sup>, Shintaro Kinugawa<sup>1</sup>, Heiner Post<sup>1</sup>, Anna Csiszar<sup>1</sup>, Pal Pacher<sup>2</sup>, Gabor Kaley<sup>1</sup> and Thomas H. Hintze<sup>1</sup>

<sup>1</sup>Department of Physiology, New York Medical College, Valhalla, NY 10595, <sup>2</sup>NIAAA, National Institutes of Health, Bethesda, MD 20892

Running title: Exercise and transcriptional analysis in male eNOS Knockout Mice

Address Correspondence:

Thomas H. Hintze, Ph.D.  
Professor, Department of Physiology  
New York Medical College  
Valhalla, NY 10595  
Phone: (914) 594-3633  
Fax: (914) 594-4108  
E-mail: [Thomas\\_Hintze@nymc.edu](mailto:Thomas_Hintze@nymc.edu)

## Abstract

Endothelium-derived nitric oxide is pivotal in regulating mitochondrial oxygen consumption and glucose uptake in mice. The aim of this study was to investigate the mechanism of age and genotype related exercise limitation in male eNOS knockout (KO) mice. 16 eNOS KO and 19 wild type (WT) male mice were used. Treadmill testing was performed at 12 months (M), 14M, 16M, 18M and 21M of age. Oxygen consumption ( $VO_2$ ), Carbon Dioxide production ( $VCO_2$ ), Respiratory Exchange Ratio (RER) and maximal running distance were determined during treadmill running. There were good linear correlations for increase of speed with increase of  $VO_2$ . The difference between KO vs. WT was not significant at 12M but was significant at 18M. Linear regression showed KO mice consumed more oxygen at the same absolute and relative workload suggesting that the inhibition of oxygen consumption by NO was not present in KO mice. KO mice performed 30-50% less work than WT mice at each age (work=vertical distance\* weight). In contrast to WT, the work performed by KO significantly decreased from  $17 \pm 1.4$  mkg at 12M to  $9.4 \pm 1.7$  mkg at 21M. Running distance (RD) was significantly decreased from  $334 \pm 27$  m at 12M to  $178 \pm 38$  m at 21M and the  $VO_{2max}$ ,  $VCO_{2max}$  and  $RER_{max}$  per work unit were significantly higher in KO compared with WT. Using gene arrays, there was evidence of a fetal phenotype in KO at 21M. In conclusion, there are age and genotype related exercise limitations in maximal work performed and maximal running distance in male eNOS KO mice indicative of the fetal phenotype and age related onset of heart failure.

Key words:  $VO_{2max}$ , RER, Work, eNOS knockout, microarray

## Introduction

Nitric oxide has been well known as a potent vascular smooth muscle relaxant and regulator of cardiovascular homeostasis. NO can modulate glucose uptake (54) in mice and substrate utilization in conscious dogs with overt heart failure (44). We have reported that basal cardiac production of NO falls during cardiac decompensation, and this is associated with a significant increase in myocardial glucose uptake and decrease in free fatty acid (FFA) utilization (44). Our previous studies demonstrated that NO inhibits mitochondrial oxygen consumption in mouse heart (35), dog skeletal muscle (50) and humans (34). We have suggested that endogenous endothelial nitric oxide synthase-derived nitric oxide is a physiological regulator of myocardial oxygen consumption (35).

During exercise, there is a significant increase in the release of NO from the coronary circulation in conscious dogs, and there are greater increases in total oxygen consumption, and oxygen consumption in skeletal muscle and in the heart when NO synthesis is blocked. Thus, NO plays a role in matching blood flow to tissue metabolism at rest and during exercise (61). Conditions of reduced EDNO synthesis or activity (e.g., heart failure) result in an inadequate exercise hyperemic response that is rate limiting for oxygen transport and exercise capacity. In normal mice, L-arginine enhances exercise-induced EDNO synthesis and aerobic capacity (37). Dyke et al. (12) reported a diminution of forearm exercise hyperemia during prolonged handgrip exercise in humans with infusion of NOS inhibitor.

Laboratory mice are frequently used in aging research and in exercise physiology. One study demonstrated that in untrained C57BL/6J mice  $VO_{2max}$  and maximal exercise capacity declined with age (48). Cross-sectional and longitudinal studies in humans and

in rats have demonstrated similar changes in  $\text{VO}_2$  max associated with increasing age (19, 23, 39). Findings in several different mammalian species strongly support the hypothesis that maximal  $\text{O}_2$  consumption and maximal exercise capacity both decline as a direct result of aging (20).

Mice lacking endothelial nitric oxide synthase have been generated. There is an increase in oxygen consumption and glucose uptake (54) in eNOS KO mouse hearts (35). Our previous data indicate that there is cardiac dysfunction in male eNOS KO mice with age (31). No study has been done to address the potential limitation in exercise capacity and its molecular basis in those mice with age. Therefore, the aims of this study were to investigate age and genotype related exercise limitation in:  $\text{VO}_2$ max,  $\text{VCO}_2$ max, RERmax, work performed and maximal running distance attained by male eNOS KO and WT mice. We hypothesized that eNOS KO mice would perform less work and run a shorter distance than wild type mice with age. The potential molecular basis of these differences was determined using gene arrays.

## **Materials and Methods**

### **Animals Studied**

Heterozygote eNOS KO mice, originally developed by Shesely et al. (51) , were interbred to generate eNOS +/-, homozygous KO, and wild-type WT mice. Mice were genotyped by Southern blot analysis of DNA from tail snips as described previously (51). 16 male KO and 19 male WT mice were used in this study. All protocols were approved by the Institutional Animal Care and Use Committee of New York Medical College and conform to the current National Institutes of Health and American Physiological Society guidelines for the use and care of laboratory animals.

### **Equipment**

The Columbus Instruments Oxymax system and Columbus Instruments Eco 3/6 Treadmill were used in this study. The system monitors oxygen and carbon dioxide gas fractions at both the inlet and output ports of test chambers to calculate O<sub>2</sub> consumption, CO<sub>2</sub> production and respiratory exchange ratio (RER). The respiratory exchange ratio (RER) is the ratio between the carbon dioxide production and the oxygen consumption. Work was calculated as vertical distance\* weight.

### **Experimental protocol**

Each mouse was given one practice trial three days before the experiment at speed 10 m/min for 10 mins to adapt to the testing environment. The mice had free access to water but no food 3 hours before the experiment. The mice were weighed and placed onto treadmill for a 15-min period of acclimation. VO<sub>2</sub>, VCO<sub>2</sub> and RER were measured during rest, exercise, and for at least 5 mins during recovery after the running. Distance run until exhaustion was measured. Mice ran at a constant 10° angle. We increased the running

speed at 2-min intervals by 2m/min until the mouse was exhausted. Exhaustion was defined as spending time on the shocker plate without attempting to reengage the treadmill within 10 seconds. The experiments were performed when the KO and WT mice were  $12.5\pm 0.2$ ,  $14.2\pm 0.3$ ,  $16.5\pm 0.1$ ,  $18.3\pm 0.2$  and  $21.5\pm 0.5$  months old. During this study, 6 KO mice died so that only the healthiest survived. There were no deaths in the WT.

### **Statistical analysis**

For the statistical analyses the average  $VO_2$  (expressed as ml/kg/min) at each speed at 12M and 18M for both KO and WT mice was determined. Linear regression of  $VO_2$  as a function of treadmill speed and linear regression of work performed and maximal running distance with age and comparison of linear regressions between KO and WT group were conducted using Sigmastat and NCSS 2000-PASS 2000 software. The comparison of both genotypes for  $VO_{2max}$ ,  $VCO_{2max}$  and  $RER_{max}$  was performed via two way analysis of variance (ANOVA) to determine the main effect of age and genotype on oxygen uptake. All data were presented as mean  $\pm$  standard error.  $P < 0.05$  was accepted as level of significance.

### **RNA isolation**

Total RNA was extracted from the left ventricle from eNOS male KO (n=3) and WT (n=4) mice at the age of 21M. RNA was extracted with a commercial RNA isolation kit using Trizol (TRI REAGENT, Sigma, Saint Louis Missouri) followed by the RNeasy total RNA extraction kit with modifications made by the URMFC FGC (detailed protocol at <http://fgc.urmc.rochester.edu/>). RNA quality was assessed by electrophoresis using the Agilent Bioanalyzer 2100.

### **Microarray labeling and hybridization**

Between 1 and 10 $\mu$ g of total RNA from each sample was used to generate a high fidelity cDNA, which is modified at the 3' end to contain an initiation site for T7 RNA polymerase. Upon completion of cDNA synthesis 1 $\mu$ g of product was used in an *in vitro* transcription (IVT) reaction that contains biotinylated UTP and CTP which are utilized for detection following hybridization to the oligonucleotide microarray. 20 $\mu$ g of full-length cRNA, from both control and enriched samples, was fragmented in 200mM Tris-acetate (pH 8.1), 500 mM KOAc and 150 mM MgOAc at 94° C for 35 minutes. Following fragmentation all components generated throughout the processing procedure (cDNA, full-length cRNA, and fragmented cRNA) were analyzed by electrophoresis using the Agilent Bioanalyzer 2100 to assess the appropriate size distribution prior to microarray hybridization. Detailed protocols for sample preparation using the Affymetrix labeling protocols can be found at <http://www.affymetrix.com>.

Each cRNA was hybridized to an individual Affymetrix GeneChip Mouse Expression Array 430A, which was subsequently processed and scanned according to the manufacturer's instructions. Each array quantifies the expression level of 39,000 transcripts and variants, including over 34,000 well substantiated mouse genes (<http://www.affymetrix.com>). The cDNA array hybridizations and scanning were carried out by Dr. Andrew Brooks, Director of the Functional Genomics Center at the University of Rochester Medical Center through the AMDec consortium collaboration. Detailed protocols are available at <http://fgc.urmc.rochester.edu/>.

### **Microarray data analysis**

All arrays referred to in this study were assessed for “array performance” prior to data analysis. This process involved the statistical analysis of control transcripts that are spiked into the samples themselves and the hybridization cocktail to assess array performance. In addition, several genes have been identified on each array to help assess the overall quality of signal intensity from all arrays. The results of this analysis were helpful to validate the reproducibility of each array at baseline allowing us to define the lower level of sensitivity that was employed to identify small changes in biologically relevant genes.

Prior to analysis, data from each hybridization were processed using Microarray Suite software, v 5.0 (MAS 5.0) to yield average difference values corresponding to signal intensity for each probe-set. Distinct algorithms were used to determine the absolute call, which distinguishes the presence or absence of a transcript, the differential change in gene expression (increase (I), decrease (D), marginal increase (MI), marginal decrease (MD), and no change (NC)), and the magnitude of change, which is represented as signal log ratio (on a log base 2 scale). T-tests were performed on the normalized signal values prior to exploring additional analyses.

All the hybridization data have been submitted to the National Center for Biotechnology Information (NCBI) Gene Expression Omnibus database (GEO: <http://www.ncbi.nlm.nih.gov/geo>) with GEO Accession Numbers for series GSE1988. The raw pixels data was imported into GeneTraffic MULTI and all subsequent analyses were performed on a GeneTraffic server (GeneTraffic v. 3.0-27, Iobion Informatics, La Jolla, CA) at the Functional Genomics Core Facility of New York Medical College. All the microarray data were analyzed and normalized using a Robust Multi-Chip Analysis

algorithm (RMA). The average of all the wild type data set was used as the baseline for the analysis.

The expression data generated from GeneTraffic was then imported into PathwayAssist software version 2.53 (Iobion Informatics, La Jolla, CA). We visualized and explored biological association networks (BAN) represented in the ResNet™ database. Microarray gene expression data was overlaid on a BAN to show how genes are affected in eNOS KO mice.

### **Statistical Analysis**

Statistical significance for changes in gene expression was also performed in GeneTraffic using a two-class method (*t*-test) and with variance stabilization. Differences were considered statistically significant at a nominal significance of  $p < 0.05$  and at least  $\pm 1.5$  fold change in expression between eNOS KO and WT mice.

### **Real-time quantitative RT-PCR**

To independently confirm the differential expression data generated by microarray analysis, real-time quantitative reverse transcription (RT)-PCR was utilized to determine the relative expression of specific genes between male KO and WT. QPCR was performed to validate changes in eight selected genes using the same RNA samples analyzed with microarrays. A relative quantitation method ( $\Delta\Delta C_t$ ) (33) was used to evaluate the relative expression of each gene between KO and WT mice. RT-PCR of GAPDH was used as an internal control and for normalization of all data.

## Results

For most of the mice, volitional running was easily maintained when the mice ran at speed from 10 to 20 m/min. Electrical shocks were necessary to keep mouse running at higher speeds.

### **VO<sub>2</sub> and percent of VO<sub>2</sub>max at each speed in KO and WT mice at 12 M**

In the range of treadmill speeds, VO<sub>2</sub> increased progressively as a function of running speed and could be expressed by simple linear equations as shown previously (13). The average VO<sub>2</sub> at each speed by KO and WT mice at 12M is shown in Figure 1A. KO increased the VO<sub>2</sub> from 33±0.74 ml/kg/min at speed of 0 to 53 ±4.4 ml/kg/min at speed of 28m/min. WT increased VO<sub>2</sub> from 42 ± 1.8 ml/kg/min at speed of 0 to 62 ± 2.7 ml/kg/min at speed of 30m/min. When we plot the linear regression, the simple linear functions are: VO<sub>2</sub> = 0.46\*speed + 37.8 for KO and VO<sub>2</sub> = 0.45\*speed + 45.6 for WT. Multiple R (correlation of actual VO<sub>2</sub> with predicted value) was 0.77 for KO and 0.88 for WT. The slopes between the two regression lines were not significantly different.

### **Maximal work performed by KO and WT mice with age**

KO mice slightly lost weight from 30±0.8g at 12M to 29±0.5g at 18M, whereas WT gained weight from 31±1g at 12M to 33±0.9g at 18M. At 12M, KO mice weighed about 3% less than WT and this difference was not significant. But at 18M, KO weighed significantly less than WT by about 12% (p<0.05). KO performed 30-50% less work compared to WT at each age. As shown in Figure 1B, in WT work performed with age did not change (24 ± 1.5 mkg at 12M to 22 ± 1.3 mkg at 21M, p=ns) but the work performed by KO significantly decreased (from 17±1.4 mkg at 12M to 9.4±1.7 mkg at 21M). The two way ANOVA showed the difference was significant (p<0.001). The

changes of work, between the ages of 12M to 21M for KO and WT can be described by simple linear functions:  $\text{work} = -0.79 * \text{age} + 26$  and  $\text{work} = -0.23 * \text{age} + 27$  for mice, respectively. Multiple R (correlation of actual work with predicted value) was 0.97 for KO and 0.87 for WT. The slopes between the two regression lines were significantly different ( $p < 0.01$ ) but there was no difference between the intercepts.

### **Maximal running distance by KO and WT with age**

Running distance (RD) by KO and WT with age is shown in Figure 2A. KO ran 20-60% less distance than WT at each age. WT had a significant decrease in the running distance from  $483 \pm 28.6$  m at 12M to  $369 \pm 25.7$  m at 21M and the distance run by KO was reduced from  $334 \pm 27.1$  m at 12M to  $178 \pm 38$  m at 21M ( $P < 0.05$ ). The changes of running distance, between ages of 12M to 21M for KO and WT can be described by simple linear functions:  $\text{RD} = -15.7 * \text{age} + 515$  for KO and  $\text{RD} = -9.9 * \text{age} + 568$  for WT. Multiple R was 0.96 for KO and 0.96 for WT. The slopes and constants between the two regression lines were not significantly different.

### **VO<sub>2</sub>max in KO and WT with age**

VO<sub>2</sub>max was defined as the plateau in oxygen uptake despite increasing work intensity. In cases in which a plateau was not reached, the VO<sub>2</sub>max was approximated by the peak oxygen uptake attained by the animal before exhaustion. When a further increase in treadmill speed resulted in a decline of VO<sub>2</sub> or mice refused to run, we choose the VO<sub>2</sub> as VO<sub>2</sub>max for that mouse. At age 14M, KO had a significant decrease in VO<sub>2</sub>max compared with their age-matched WT controls. At all of the other ages, there were no significant differences between these two genotypes. When the VO<sub>2</sub>max is

normalized to per work unit as shown in Figure 2B, KO have significantly higher values starting from 14M compared to WT ( $p < 0.05$ ).

#### **VCO<sub>2</sub>max in KO and WT with age**

Only at 16M and 18M, was the decrease of VCO<sub>2</sub>max in KO significant compared with their age-matched WT controls. When the VCO<sub>2</sub>max is normalized to per work unit as shown in Figure 3A, KO have higher values from 14M to 21M compared to WT ( $p < 0.05$ ).

#### **RERmax in KO and WT with age**

The RERmax was picked at the point of VO<sub>2</sub>max. There was no significant difference between KO and WT. When the RERmax is normalized to per work unit as shown in Figure 3B, KO have higher values from 12M to 21M compared to WT ( $p < 0.05$ ).

#### **Comparison of changes in gene expression between eNOS KO and WT mice**

Comparison of RNA expression levels in KO to WT revealed that of the 39,000 transcripts and variants present on the microarrays a total of 480 genes were differentially expressed at 21M ( $P < 0.05$ ). The data showed that 293 genes were expressed at significantly greater levels in eNOS KO and 187 were significantly reduced in the KO Figure 4A.

#### **Functional categories of differentially expressed genes in eNOS KO male mice**

All of the 480 genes were grouped into 7 different functional categories based on their Gene Ontology (GO) biological process annotations provided by PathwayAssist through the ResNet (tm) database. These categories are classified as cell signaling/communication/transport, cell structure/motility, metabolism, development,

immune response/apoptosis, protein/protein expression and unknown/other (Figure 4B). The results showed a wide range of distribution of expression patterns within the functional groups of genes. Shown in Figure 4B, the most-striking observation was that of the 480 genes that are differentially regulated between KO and WT, 178 encode proteins of unknown function (category unknown/other). Of genes encoding proteins of known function, the greatest number was found to be cell signaling/communication/transport, with 105 being differentially expressed. Interestingly, almost all of the differentially expressed genes within the cell structure/motility group showed increased expression in the KO. Examples of these genes are  $\alpha$ -skeletal actin, cartilage oligomeric matrix protein and myosin heavy polypeptide 7 which were up-regulated by 5.90, 4.96 and 3.53 fold respectively in KO. The other functional category for which a substantial number of genes are differentially regulated is metabolism; 29 are significantly up-regulated (1.5- to 4.23-fold) and 41 are significantly down-regulated (1.5- to 7.16-fold) in KO. Many genes in the metabolism category encode proteins involved in energy metabolism and, within that group a high number of lipid metabolism genes were primarily repressed. Examples of differentially regulated metabolic genes in KO included genes encoding latent transforming growth factor beta binding protein 2, deiodinase, aminolevulinic acid synthase 2 and phosphofructokinase. These genes were up-regulated by 4.23, 2.57, 2.51 and 2.27 fold, respectively. Down regulated genes included carboxylesterase 3, methionine adenosyltransferase II, methylmalonyl-Coenzyme A mutase, deoxyuridine triphosphatase and cytosolic acyl-CoA thioesterase 1. These were down-regulated by 7.16, 2.30, 2.27, 2.25 and 2.22 fold, respectively.

In the protein/protein expression group, higher number of genes showed increased expression in KO. Most of the elevated expressions were for genes encoding enzymes involved in protein modification and degradation. In the immune response/defense/apoptosis category, 36 genes were found to be differentially expressed. Of these, 22 genes were up regulated in KO and 14 genes were down regulated. Very few genes in the category of development were found to be differentially expressed. A complete annotated list of all the genes is available in supplementary Table 1.

Heart failure is characterized at the molecular level by changes in gene expression that result in the induction of fetal genes (1). In this study, ANP was found to be significantly higher in KO (2.83 fold). BNP showed higher expression in KO but its expression was not statistically significant. In addition,  $\alpha$ -skeletal actin was significantly up regulated in KO by 5.90 fold and there was a switch from  $\alpha$ - to  $\beta$ -MyHC.  $\beta$ -MyHC was up regulated by 3.53 fold in KO.

One of the gene which was classified as unknown/other was of particular interest. This gene was designated as RIKEN cDNA A830037N07 gene (Affy ID # 1456395\_at) and it was statistically down-regulated in KO by 4.2 fold. Recent analysis of the current data showed that this gene is now been designated as peroxisome proliferative activated receptor, gamma, coactivator 1 $\alpha$  (PGC-1). Another variant of this gene on the Affymetrix chips (Affy ID # 1460336\_at) was also statistically down regulated in KO by 1.73 fold.

To more fully disclose the pathways relevant to the pathogenesis of heart failure, the 480 differentially expressed genes were grouped according to function using PathwayAssist. Of those genes, 401 were recognized by the software, and were thus subjected to subsequent analysis. The 'Find common targets for selected nodes' feature

of PathwayAssist was used to build a network of connections starting with these 401 genes and including all available categories of interaction. Some of the observed cellular processes included apoptosis, proliferation, inflammation, motility, contraction, and regeneration. This analysis highlighted the importance of these cellular processes in the development of heart failure in KO mice.

### **Correlation between microarrays and real-time RT-PCR**

Real time RT-PCR was employed to validate the final microarray data. A total of 8 different genes were selected for this analysis. There was a high correlation between expression values obtained by real-time PCR analysis and those measured by microarray analysis with  $R^2$  value of 0.91 (data not shown).

## Discussion

In the present study, we have demonstrated that the maximal work performed and running distance attained in KO were decreased significantly with age and KO have greater total oxygen consumption and run at a higher relative workload at high treadmill speed. The normalized  $\text{VO}_2\text{max}$ ,  $\text{VCO}_2\text{max}$  and  $\text{RERmax}$  to work performed was elevated in KO compared to WT with age. There was a change in genotype in KO at 21 months indicative of the development of heart failure and expression of a fetal phenotype.

At 12M and 18M, there is a good correlation for the increase of  $\text{VO}_2$  with the increase of treadmill speed. The slope of linear regression of the KO is significantly higher than that of WT at 18M. KO mice consumed more oxygen than WT especially at high speed. We also plotted the linear regression curve of the relative work load at each speed; the slopes were significantly different between these two genotypes at 18M. The genotypic differences in the slopes of the oxygen consumption of running curves observed at 18M are likely the product of the higher relative workload in WT at lower treadmill speed and higher relative workload in KO at higher treadmill speed. For example, at a treadmill speed of 16m/min WT ran at a relative workload of 62% of  $\text{VO}_2\text{max}$  and KO ran at 85% of  $\text{VO}_2\text{max}$ . Although the WT reach a higher percent of  $\text{VO}_2\text{max}$  at lower treadmill speed than KO, the  $\text{VO}_2$  required at equal relative work loads was still higher in KO. For instance, at a relative work load of 70% of  $\text{VO}_2\text{max}$ ,  $\text{VO}_2$  was  $55 \pm 5.8$  ml/kg/min for KO and  $39 \pm 3.1$  ml/kg/min for WT mice ( $P < 0.05$ ).

This increase in  $\text{VO}_2$  in KO at both absolute and relative work intensity may be due to the loss of shear stress stimulated NO regulation of mitochondrial oxygen consumption. Our previous study showed that vascular endothelium-derived NO may

play an important role in the modulation of cellular respiration and O<sub>2</sub> consumption in parenchymal cells, such as skeletal and cardiac myocytes (50). The underlying mechanism is that nitric oxide can reduce the activity of a number of enzymes in the mitochondria, including: (1) aconitase, (2) NADH-ubiquinone oxidoreductase and (3) succinate-ubiquinone oxidoreductase (17, 22, 27, 46). In addition, nanomolar concentrations of NO have a significant and reversible inhibitory effect on cytochrome oxidase through a competitive binding site for O<sub>2</sub> in the enzyme (7, 9). The feed-forward mechanism is driven by the ATP metabolic products like ADP, H<sup>+</sup> and Pi to accelerate cellular respiration and O<sub>2</sub> consumption (57). In another study we showed that bradykinin had no inhibitory effect on O<sub>2</sub> consumption in heart from eNOS KO mice (35). So at high speed, WT O<sub>2</sub> consumption was regulated by NO release and this inhibition was removed in KO. During exercise at a high intensity, factors such as increased body temperature, increased energy cost of breathing, elevated blood catecholamine levels may augment oxygen consumption (10). Therefore, at high intensity exercise, KO work inefficiently compared to WT. This is further supported by the fact that inhibition of endothelium derived NO resulted in decreased myocardial metabolic efficiency, including both coupling between MVO<sub>2</sub> and cardiac performance and coupling MVO<sub>2</sub> and the ATP synthesis rate (49).

One study demonstrated that despite the increase in VO<sub>2</sub> by L-NNA in the isolated guinea pig heart at all level of contractile performance, neither the [ATP] nor the ATP synthesis rate changed (49). When NO synthesis was blocked systemically in the resting dogs, there was an elevation in total body oxygen consumption, which was accompanied by an elevation in body temperature (4).

Unlike at 18M, there was no difference between the slopes of the linear regressions for either the absolute and relative workload of KO and WT at 12M. There may be some compensatory mechanism working at 12M to block the effect of gene deletion but age uncovered the consequence of eNOS deletion. Indeed studies already demonstrated that increased release of prostaglandins contributes to flow-induced arteriolar dilation in young eNOS KO mice (53) and shear stress can activate endothelial nNOS to release NO compensating for the absence of eNOS-derived NO in coronary arteries of young KO mice (24).

Treadmill exercise has typically been the choice for exercise involving mice. Generally, treadmill running at 4m/min with an 18° slope has been termed “submaximal” intensity (14) , whereas running at 12 m/min with an 8° slope has been characterized as “moderate”-intensity exercise (5) . Our mice could achieve at least 28m/min speed with 10° slope until exhaustion.

Knockout mice performed 30-50% less work than WT at each age. WT slightly decrease the work performed with age by rate of 0.8% per month. But the work performed by KO decreased much faster, 5% per month. KO ran 20-60% shorter distance than WT at each age. WT decrease 23% of the running distance from 12M to 21M whereas the running distance of KO was shortened by 47% ( $p < 0.001$ ). That maximal exercise capacity declines with age has been shown in several studies in aged mice (48), in dogs (20), and rats (39). In addition, our previous study (31) found that KO developed cardiac dysfunction between 14M and 21M, which is responsible for the mortality we observed and may account for the marked decrease of work and running distance.

Maxwell et al showed that endothelium-derived nitric oxide (EDNO) contributes to exercise hyperemia and is a determinant of aerobic capacity in exercising mice (38). They also indicate that exercise capacity depends on the integrity of the NOS pathway (37). When the deletion of eNOS gene is added to aging there is a decrease in the exercise capacity. In KO mice the mitochondrial oxygen consumption was elevated and a failure to reduce leg vascular resistance may limit the increase in leg blood flow. Consequently, perfusion in the exercising limb is unable to keep up with the rising demand for O<sub>2</sub> transport, the balance between supply and metabolism is severely compromised.

There are several studies indicating that the VO<sub>2</sub>max declines with age: Schefer et al indicated that VO<sub>2</sub>max declined with age in mice. A decline in maximal oxygen consumption of about 10% per decade after 30 years of age has been observed in studies of a healthy humans (18) and Lawler et al. demonstrated that the oxygen cost of treadmill running is lower for 24-month-old rats than in 4-month-old rats except at high work levels (28) . In our study we only found a slight decrease in VO<sub>2</sub>max from 63±3.4 ml/kg/min at 12M to 60ml/kg/min at 21M in WT. The discrepancies may be explained in that the age ranges in our investigation i.e. 9M is not long enough for normal mice to present a significant aging effect.

Only at age 14M for VO<sub>2</sub>max and at 16M and 18M for VCO<sub>2</sub>max, did KO have significant decrease compared with their age-matched WT controls. Since the KO and WT were not at the same workload and not at the same cumulative distance run at the point at which we chose the values for VO<sub>2</sub>max, VCO<sub>2</sub>max and RERmax, this way of evaluating the data may not be appropriate. We therefore normalized the data to per work

unit and per running distance. KO have significantly higher values from 14M to 21M for  $VO_2\text{max}$ ,  $VCO_2\text{max}$  compared to WT ( $p < 0.05$ ).

KO mice had a significant elevation in the  $VO_2$  at 14M compared to WT, this correlated with our previous study showing that starting from 14M, KO have significant cardiac hypertrophy and that cardiac function was markedly reduced at 21M (31).

$VCO_2$  also started to rise after 14M. Several previous studies showed that NO can regulate substrate utilization. Glucose uptake was increased in KO mice and mice with L-NAME in a Langendorff heart preparation (54). Blockade of NO synthesis resulted in reductions in myocardial FFA consumption for comparable levels of cardiac work (4). The acute inhibition of NO synthase by NLA causes a switch from fatty acids to lactate and glucose utilization by the heart which can be reversed by a NO donor (45). Basal cardiac production of NO falls below normal levels during cardiac decompensation and there are shifts in substrate utilization from fatty acids to glucose. It has been demonstrated *in vitro* that NO can stimulate ADP-ribosylation of glyceraldehyde-3-phosphate dehydrogenase (60). This may inhibit enzyme activity. This augmented glucose utilization may account for the results of the current study i.e. that the  $VCO_2\text{max}$  and  $RER\text{max}$  were significantly elevated in KO compared to the WT. ATP yield from carbohydrate oxidation is greater for a given rate of oxygen consumption because of the higher ATP/ $O_2$  ratio compared with that of fatty acid oxidation (52).

Data from Ji et al. (26) reveal that a brief acclimation period in untrained animals does not affect the activity of working muscle metabolic enzymes. An increase in stride length and consequent reduction of stride rate could result in a lower oxygen cost of running (55). Oxygen consumption is total body  $VO_2$  and during exercise, most of the  $O_2$

was consumed by skeletal muscle. One limitation of this study is that we could not exclude the skeletal muscle lean mass difference between these two groups. The body mass of KO is significantly less than WT at 18M, but if we assume that the lean skeletal muscle mass follow the decrease in body mass, KO should consume less oxygen whereas in our study the  $VO_2$  of KO is significantly higher, further supporting the change in mitochondrial oxygen consumption and substrate utilization due to gene deletion contributed here.

The study presented here showed that the work performed by KO significantly decreased with age beginning at 12M. In addition, in our previous data there was cardiac dysfunction in KO mice with age and 50% mortality at 21M. In the current study 6 out of 16, 40 % of KO died by 21 M. Therefore, it was of interest to investigate the gene expression profile of aged KO in comparison to WT in order to explore the genetic markers and molecular mechanisms leading to heart failure. The array data presented showed that the gene profile in our 21M old KO is indicative of cardiac failure and remodeling. 480 genes grouped into 7 different functional categories were found to have altered expression in KO mice. These categories are classified as cell signaling/communication/transport, cell structure/motility, metabolism, development, immune response/apoptosis, protein/protein expression and unknown/other.

Previous studies have shown that heart failure is characterized at the molecular level by changes in gene expression that result in the repression of adult genes, such as  $\alpha$ -myosin heavy chain ( $\alpha$ MyHC) and SERCA2A, and the induction of fetal genes (1). The change in MyHC expression is a logical candidate for affecting cardiac contractility, since small changes in isoform composition have been shown to affect contractility of cardiac

myocytes. ANP was found to be significantly higher in KO (2.83 fold). BNP showed higher expression in KO but this was not statistically significant. In addition,  $\alpha$ -skeletal actin was significantly upregulated in KO by 5.90 fold and there was a switch from  $\alpha$ - to  $\beta$ -MyHC (myosin heavy chain).  $\beta$ -MyHC was up regulated by 3.53 fold in KO.

Oxidative stress may play an important role in the pathophysiology of heart failure. Previous studies have shown that the overexpression of glutathione peroxidase (Gpx3) attenuates left ventricular (LV) remodeling and failure after myocardial infarction (MI). In our study Gpx3 was significantly upregulated by 2.33 fold in KO. Some studies have reported that the yeast prion protein Ure2 shows glutathione peroxidase activity in both native and fibrillar forms (3). In our study prion protein was also significantly upregulated by 1.85 fold in KO.

It has been well established that fatty acids are primary fuels for energy production in healthy hearts. However, in disease states, glucose becomes the favored energy source. Our data indicate that there might be an adaptation in expression of fatty acid metabolism genes as a means to accomplish this metabolic reprogramming. The up regulation of some of the genes which are involved in glucose metabolism (phosphofructokinase, 2,3-bisphosphoglycerate mutase, protein phosphatase 1, hexokinase 1, amylo-1,6-glucosidase, 4-alpha-glucanotransferase and glucose phosphate isomerase 1) and the down regulation of several lipid metabolism genes (carboxylesterase 3, phospholipase A2, cytosolic acyl-CoA thioesterase 1 and short chain acyl-Coenzyme A dehydrogenase) may be a reflection of altered bioenergetics in a failing heart in KO.

Another interesting observation is that the peroxisome proliferative activated receptor, gamma, coactivator 1 (PGC-1) gene was statistically down-regulated in KO by

4.2 fold. Recently, the peroxisome proliferator-activated receptor (PPAR)  $\gamma$ coactivator-1 $\alpha$  (PGC-1 $\alpha$ ) has been identified as an inducible upstream regulator of mitochondrial number and function (29,58). Recent studies implicated PGC-1 $\alpha$  in the activation of the mitochondrial biogenesis program in both heart and skeletal muscle (58). Another study by Garnier et al (15) has shown that the expression of the peroxisome proliferator activated receptor gamma co-activator 1 $\alpha$  (PGC-1 $\alpha$ ) gene was significantly downregulated in congestive heart failure (CHF) and that PGC-1 $\alpha$  correlated with the oxidative capacity in failing cardiac and skeletal muscles as well as in healthy muscles. Therefore, the decreased oxidative capacity in cardiac and skeletal muscles in CHF may eventually result from a decrease in mitochondrial gene expression linked to PGC-1 $\alpha$  (15). Sano et al (47) have also shown that impaired transcription of PGC-1 and its targets likely contributes to the transition to heart failure, via mitochondrial dysfunction and, at least in part, the resulting vulnerability to apoptosis.

In heart, PGC-1 $\alpha$  expression increases sharply at birth coincident with a perinatal shift from glucose metabolism to fat oxidation. Consistent with its emerging role as a central regulator of energy metabolism, PGC-1 $\alpha$  is abundantly expressed in mitochondrial-rich tissues such as heart, skeletal muscle, and brown adipose tissue (42). PGC-1 $\alpha$  expression is inducible in these tissues in response to physiological stimuli. In heart and skeletal muscle, physiological stimuli, including fasting and exercise, lead to an increase in PGC-1 $\alpha$  gene expression (29, 16, 2); conversely, pressure overload decreases PGC-1 $\alpha$  expression (30). Signaling pathways associated with these stimuli, including p38 MAP kinase,  $\beta$ -adrenergic/cAMP, nitric oxide, AMP kinase, and Ca<sup>2+</sup>-calmodulin kinase, activate PGC-1 $\alpha$ , and its downstream target genes either by increasing PGC-1 $\alpha$  expression

or transactivation function (43, 59, 6, 41) . At the present time nothing is known regarding the signaling pathways leading to a downregulation of PGC-1 and decreased energy metabolism in CHF. One proposed theory by Garnier et al (15) was that mitogen-activated protein kinases as well as the protein kinase Akt or protein kinase B (PKB) pathways, which are not activated in hypertrophied heart, are highly activated in heart failure irrespective of the cause of the disease (21).  $\text{TNF}\alpha$ , angiotensin II and endothelin-1, which are dramatically increased in heart failure, may potentially activate the Akt pathway (40). Cardiac-specific expression of a constitutively active mutant of Akt mediates a nearly threefold downregulation of PGC-1 $\alpha$  mRNA expression (11). Overexpression of  $\text{TNF}\alpha$  induces heart failure, accompanied by mitochondrial abnormalities and impaired DNA repair activity (32) and  $\text{TNF}\alpha$  has been proposed to play a contributory role in mitochondrial defects in CHF (36). This provides a possible link between neurohumoral activation, decreased PGC-1 $\alpha$  expression, and altered cardiac and skeletal muscle bioenergetics in CHF.

One of the limitations of this study is that eNOS KO are hypertensive and develop cardiac hypertrophy with age. Because of this, it might be difficult to differentiate the specific changes in gene expression due to the absence of NO generated by eNOS from those associated with the pressure overload phenotype in these mice. However, in our previous study (31), we have shown that female eNOS KO maintain an elevated blood pressure for 21M and yet they do not develop cardiac dysfunction as seen in male KO. Therefore, it is unlikely that changes in gene expression found in hearts of KO male mice are simply due to pressure overload.

A recent study by Cappola et al (8) described the cardiac expression profiles using Affymetrix mouse arrays (MG-U74A) from eNOS KO and nNOS KO. There was a limited overlap between the genes identified in their eNOS KO studies and those in our data set. The limited correspondence between the two data sets may be a result of substantial differences in array design and disease state. Most sequences previously represented on the GeneChip Murine Genome U74Av2 Array are represented on the GeneChip Mouse Expression Array 430A. Due to the dynamic nature of public databases, probe sets for these sequences are not identical and in some cases are represented by a completely new probe set. As a result, data generated with different versions of the mouse arrays may not always produce concordant results (<http://www.affymetrix.com>). In addition, in their study, both eNOS KO and nNOS KO models showed similar hypertrophic cardiac phenotypes. In our recent study we have found that eNOS KO have a reduced life expectancy, due to the development of dilated cardiomyopathy (56). The eNOS KO model used in their study was generated by Huang et al (25); we are using eNOS KO generated by Shesely et al (51).

In conclusion, there are age and genotype related exercise limitations in work performed and maximal running distance attained in KO. The genotype difference in the slopes of the oxygen consumption running curves at absolute and relative workload observed in this study demonstrate that KO produce work less efficiently and consume more oxygen compared to WT. Starting from 14M, the normalized  $\text{VO}_2\text{max}$ ,  $\text{VCO}_2\text{max}$  began to increase significantly, which correlated with the time-course of cardiac dysfunction, implicating an inefficiency of oxygen consumption and increase in skeletal muscle oxygen consumption in KO. This may be compounded by the switching over of

substrate utilization from fatty acids to glucose due to the deletion of eNOS gene and which was uncovered with age.

**Grants**

WL was supported by a pre-doctoral fellowship (#0215297T) from the NYS affiliate of the American Heart Association. HP was supported by Grant PO 672/1-1 from the Germany Research Federation. Work was supported by PO-43023, HL 50142 and HL 61029 (THH).

## References

1. **Abraham WT, Gilbert EM, Lowes BD, Minobe WA, Larrabee P, Roden RL, Dutcher D, Sederberg J, Lindenfeld JA, Wolfel EE, Shakar SF, Ferguson D, Volkman K, Linseman JV, Quaife RA, Robertson AD, and Bristow MR.** Coordinate changes in myosin heavy chain isoform gene expression are selectively associated with alterations in dilated cardiomyopathy phenotype. *Mol Med* 8:750-760, 2002.
2. **Baar K, Wende AR, Jones TE, Marison M, Nolte LA, Chen M, Kelly DP, and Holloszy JO.** Adaptations of skeletal muscle to exercise: Rapid increase in the transcriptional coactivator PGC-1 $\alpha$ . *FASEB J* 16: 1879–1886, 2002.
3. **Bai M, Zhou JM, and Perrett S.** The yeast prion protein Ure2 shows glutathione peroxidase activity in both native and fibrillar forms. *J Biol Chem*. Published on September 15, 2004 as Manuscript M406612200.
4. **Bernstein RD, Ochoa FY, Xu X, Forfia P, Shen W, Thompson CI, and Hintze TH.** Function and production of nitric oxide in the coronary circulation of the conscious dog during exercise. *Circ Res* 79: 840-848, 1996.
5. **Blank SE, Johansson JO, Origines MMT, and Meadows GG.** Modulation of NK cell activity by moderate intensity endurance training and chronic ethanol consumption. *J Appl Physiol* 72: 8-14, 1992.
6. **Boss O, Bachman E, Vidal-Puig A, Zhang C-Y, Peroni O, Lowell BB.** Role of the  $\beta_3$ -Adrenergic receptor and/or putative  $\beta_4$ -Adrenergic receptor on the expression of uncoupling proteins and peroxisome proliferator-activated receptor- $\gamma$  coactivator-1. *Biochem Biophys Res Commun* 261: 870–876, 1999.

7. **Brown GC, Bolanos JP, Heales SJ, and Clark JB.** Nitric oxide produced by activated astrocytes rapidly and reversibly inhibits cellular respiration. *Neurosci Lett* 193: 201-204, 1995.
8. **Cappola TP, Cope L, Cernetich A, Barouch LA, Minhas K, Irizarry RA, Parmigiani G, Durrani S, Lavoie T, Hoffman EP, Ye SQ, Garcia JG, and Hare JM.** Deficiency of different nitric oxide synthase isoforms activates divergent transcriptional programs in cardiac hypertrophy. *Physiol Genomics* 14: 25-34, 2003.
9. **Cleeter MW, Cooper JM, Darley-USmar VM, Moncada S, and Schapira AH.** Reversible inhibition of cytochrome c oxidase, the terminal enzyme of the mitochondrial respiratory chain, by nitric oxide. Implications for neurodegenerative diseases. *FEBS Lett* 345: 50-54, 1994.
10. **Coast JR and Krause KM.** Relationship of oxygen consumption and cardiac output to work of breathing. *Med Sci Sports Exerc* 25: 335-340, 1993.
11. **Cook SA, Matsui T, Li L & Rosenzweig A.** Transcriptional effects of chronic Akt activation in the heart. *J Biol Chem* 277: 22528-22533, 2002.
12. **Dyke CK, Proctor DN, Dietz NM, and Joyner MJ.** Role of nitric oxide in exercise hyperaemia during prolonged rhythmic handgripping in humans. *J Physiol* 488: 259-265, 1995.
13. **Fernando P, Bonen A, and Hoffman-Goetz L.** Predicting submaximal oxygen consumption during treadmill running in mice. *Can J Physiol Pharmacol* 71: 854-857, 1993.

14. **Fowler WM, Jr., Abresch RT, Larson DB, Sharman RB, and Entrikin RK.** High-repetitive submaximal treadmill exercise training: effect on normal and dystrophic mice. *Arch Phys Med Rehabil* 71: 552-557, 1990.
15. **Garnier A, Fortin D, Delomenie C, Momken I, Veksler V, and Ventura-Clapier R.** Depressed mitochondrial transcription factors and oxidative capacity in rat failing cardiac and skeletal muscles. *J Physiol* 551(Pt 2):491-501, 2003.
16. **Goto M, Terada S, Kato M, Katoh M, Yokozeki T, Tabata I, and Shimokawa T.** cDNA cloning and mRNA analysis of PGC-1 in epitrochlearis muscle in swimming-exercised rats. *Biochem Biophys Res Commun* 274: 350–354, 2000.
17. **Granger DL and Lehninger AL.** Sites of inhibition of mitochondrial electron transport in macrophage- injured neoplastic cells. *J Cell Biol* 95: 527-535, 1982.
18. **Hagberg JM.** Effect of training on the decline of VO<sub>2</sub>max with aging. *Fed Proc* 46: 1830-1833, 1987.
19. **Hagberg JM, Allen WK, Seals DR, Hurley BF, Ehsani AA, and Holloszy JO.** A hemodynamic comparison of young and older endurance athletes during exercise. *J Appl Physiol* 58: 2041-2046, 1985.
20. **Haidet GC.** Dynamic exercise in senescent beagles: oxygen consumption and hemodynamic responses. *Am J Physiol* 257: H1428-1437, 1989.
21. **Haq S, Choukroun G, Lim H, Tymitz KM, Del Monte F, Gwathmey J, Grazette L, Michael A, Hajjar R, Force T and Molkenstin JD.** Differential activation of signal transduction pathways in human hearts with hypertrophy versus advanced heart failure. *Circulation* **103**: 670-677, 2001.

22. **Hibbs JB, Jr., Taintor RR, and Vavrin Z.** Macrophage cytotoxicity: role for L-arginine deiminase and imino nitrogen oxidation to nitrite. *Science* 235: 473-476, 1987.
23. **Higginbotham MB, Morris KG, Williams RS, Coleman RE, and Cobb FR.** Physiologic basis for the age-related decline in aerobic work capacity. *Am J Cardiol* 57: 1374-1379, 1986.
24. **Huang A, Sun D, Shesely EG, Levee EM, Koller A, and Kaley G.** Neuronal NOS-dependent dilation to flow in coronary arteries of male eNOS-KO mice. *Am J Physiol Heart Circ Physiol* 282: H429-436, 2002.
25. **Huang PL, Dawson TM, Bredt DS, Snyder SH, Fishman MC.** Targeted disruption of the neuronal nitric oxide synthase gene. *Cell* 75: 1273 -1286, 1993.
26. **Ji LL, Stratman FW, and Lardy HA.** Enzymatic down regulation with exercise in rat skeletal muscle. *Arch Biochem Biophys* 263: 137-149, 1988.
27. **Lancaster JR, Jr. and Hibbs JB, Jr.** EPR demonstration of iron-nitrosyl complex formation by cytotoxic activated macrophages. *Proc Natl Acad Sci U S A* 87: 1223-1227, 1990.
28. **Lawler JM, Powers SK, Hammeren J, and Martin AD.** Oxygen cost of treadmill running in 24-month-old Fischer-344 rats. *Med Sci Sports Exerc* 25: 1259-1264, 1993.
29. **Lehman JJ, Barger PM, Kovacs A, Saffitz JE, Medeiros D, and Kelly DP.** PPAR $\gamma$  coactivator-1 (PGC-1) promotes cardiac mitochondrial biogenesis. *J Clin Invest* 106: 847-856, 2000.

30. **Lehman JJ, and Kelly DP.** Transcriptional activation of energy metabolic switches in the developing and hypertrophied heart. *Clin Exp Pharmacol Physiol* 29:339-45, 2002.
31. **Li W, Mital S, Ojaimi C, Csiszar A, Kaley G, Hintze TH.** Premature death and age-related cardiac dysfunction in male eNOS-knockout mice. *J Mol Cell Cardiol* 37: 671-680, 2004.
32. **Li YY, Chen D, Watkins SC and Feldman AM.** Mitochondrial abnormalities in tumor necrosis factor-alpha-induced heart failure are associated with impaired DNA repair activity. *Circulation* 104: 2492-2497, 2001.
33. **Livak KJ and Schmittgen TD.** Analysis of relative gene expression data using real-time quantitative PCR and the 2<sup>(-Delta Delta C(T))</sup> Method. *Methods* 25: 402-408, 2001.
34. **Loke KE, Laycock SK, Mital S, Wolin MS, Bernstein R, Oz M, Addonizio L, Kaley G, and Hintze TH.** Nitric oxide modulates mitochondrial respiration in failing human heart. *Circulation* 100: 1291-1297, 1999.
35. **Loke KE, McConnell PI, Tuzman JM, Shesely EG, Smith CJ, Stackpole CJ, Thompson CI, Kaley G, Wolin MS, and Hintze TH.** Endogenous endothelial nitric oxide synthase-derived nitric oxide is a physiological regulator of myocardial oxygen consumption. *Circ Res* 84: 840-845, 1999.
36. **Marin-Garcia J, Goldenthal MJ and Moe GW.** Abnormal cardiac and skeletal muscle mitochondrial function in pacing- induced cardiac failure. *Cardiovasc Res* 52: 103-110, 2001.

37. **Maxwell AJ, Ho HV, Le CQ, Lin PS, Bernstein D, and Cooke JP.** L-arginine enhances aerobic exercise capacity in association with augmented nitric oxide production. *J Appl Physiol* 90: 933-938, 2001.
38. **Maxwell AJ, Schauble E, Bernstein D, and Cooke JP.** Limb blood flow during exercise is dependent on nitric oxide. *Circulation* 98: 369-374, 1998.
39. **Mazzeo RS, Brooks GA, and Horvath SM.** Effects of age on metabolic responses to endurance training in rats. *J Appl Physiol* 57: 1369-1374, 1984.
40. **Molkentin JD, and Dorn GW II.** Cytoplasmic signaling pathways that regulate cardiac hypertrophy. *Annu Rev Physiol* 63: 391-426, 2001.
41. **Nisoli E, Clementi E, Paolucci C, Cozzi V, Tonello C, Sciorati C, Bracale R, Valerio A, Francolini M, Moncada S, and Carruba MO.** Mitochondrial biogenesis in mammals: The role of endogenous nitric oxide. *Science* 299: 896–899, 2003.
42. **Puigserver P, Wu Z, Park CW, Graves R, Wright M, and Spiegelman BM.** A cold-inducible coactivator of nuclear receptors linked to adaptive thermogenesis. *Cell* 92: 829–839, 1998.
43. **Puigserver P, Rhee J, Lin J, Wu Z, Yoon JC, Zhang C-Y, Krauss S, Mootha VK, Lowell BB, and Spiegelman BM.** Cytokine stimulation of energy expenditure through p38 MAP kinase activation of PPAR $\gamma$  coactivator-1. *Mol Cell* 8: 971–982, 2001.
44. **Recchia FA, McConnell PI, Bernstein RD, Vogel TR, Xu X, and Hintze TH.** Reduced nitric oxide production and altered myocardial metabolism during the

- decompensation of pacing-induced heart failure in the conscious dog. *Circ Res* 83: 969-979, 1998.
45. **Recchia FA, McConnell PI, Loke KE, Xu X, Ochoa M, and Hintze TH.** Nitric oxide controls cardiac substrate utilization in the conscious dog. *Cardiovasc Res* 44: 325-332, 1999.
46. **Reif DW and Simmons RD.** Nitric oxide mediates iron release from ferritin. *Arch Biochem Biophys* 283: 537-541, 1990.
47. **Sano M, Wang SC, Shirai M, Scaglia F, Xie M, Sakai S, Tanaka T, Kulkarni PA, Barger PM, Youker KA, Taffet GE, Hamamori Y, Michael LH, Craigen WJ, and Schneider MD.** Activation of cardiac Cdk9 represses PGC-1 and confers a predisposition to heart failure. *EMBO J* 23:3559-69, 2004.
48. **Schefer V and Talan MI.** Oxygen consumption in adult and AGED C57BL/6J mice during acute treadmill exercise of different intensity. *Exp Gerontol* 31: 387-392, 1996.
49. **Shen W, Tian R, Saupe KW, Spindler M, and Ingwall JS.** Endogenous nitric oxide enhances coupling between O<sub>2</sub> consumption and ATP synthesis in guinea pig hearts. *Am J Physiol Heart Circ Physiol* 281: H838-846, 2001.
50. **Shen W, Xu X, Ochoa M, Zhao G, Bernstein RD, Forfia P, and Hintze TH.** Endogenous nitric oxide in the control of skeletal muscle oxygen extraction during exercise. *Acta Physiol Scand* 168: 675-686, 2000.
51. **Shesely EG, Maeda N, Kim HS, Desai KM, Krege JH, Laubach VE, Sherman PA, Sessa WC, and Smithies O.** Elevated blood pressures in mice lacking

- endothelial nitric oxide synthase. *Proc Natl Acad Sci U S A* 93: 13176-13181, 1996.
52. **Stanley WC, Lopaschuk GD, Hall JL, and McCormack JG.** Regulation of myocardial carbohydrate metabolism under normal and ischaemic conditions. Potential for pharmacological interventions. *Cardiovasc Res* 33: 243-257, 1997.
53. **Sun D, Huang A, Smith CJ, Stackpole CJ, Connetta JA, Shesely EG, Koller A, and Kaley G.** Enhanced release of prostaglandins contributes to flow-induced arteriolar dilation in eNOS knockout mice. *Circ Res* 85: 288-293, 1999.
54. **Tada H, Thompson CI, Recchia FA, Loke KE, Ochoa M, Smith CJ, Shesely EG, Kaley G, and Hintze TH.** Myocardial glucose uptake is regulated by nitric oxide via endothelial nitric oxide synthase in Langendorff mouse heart. *Circ Res* 86: 270-274, 2000.
55. **Taylor CR, Heglund NC, and Maloiy GM.** Energetics and mechanics of terrestrial locomotion. I. Metabolic energy consumption as a function of speed and body size in birds and mammals. *J Exp Biol* 97: 1-21, 1982.
56. **Wahren J, Saltin B, Jorfeldt L, and Pernow B.** Influence of age on the local circulatory adaptation to leg exercise. *Scand J Clin Lab Invest* 33: 79-86, 1974.
57. **Wilson DF.** Energy metabolism in muscle approaching maximal rates of oxygen utilization. *Med Sci Sports Exerc* 27: 54-59, 1995.
58. **Wu Z, Puigserver P, Andersson U, Zhang C, Adelmant G, Mootha V, Troy A, Cinti S, Lowell B, Scarpulla RC, Spiegelman BM.** Mechanisms controlling mitochondrial biogenesis and respiration through the thermogenic coactivator PGC-1. *Cell* 98: 115-124, 1999.

59. **Wu H, Kanatous SB, Thurmond FA, Gallardo T, Isotani E, Bassel-Duby R, Williams RS.** Regulation of mitochondrial biogenesis in skeletal muscle by CaMK. *Science* 296: 349–352, 2002.
60. **Zhang J and Snyder SH.** Nitric oxide stimulates auto-ADP-ribosylation of glyceraldehyde-3- phosphate dehydrogenase. *Proc Natl Acad Sci U S A* 89: 9382-9385, 1992.
61. **Zhao G, Bernstein RD, and Hintze TH.** Nitric oxide and oxygen utilization: exercise, heart failure and diabetes. *Coron Artery Dis* 10: 315-320, 1999.

## Figure Legends

**Figure 1A:** The average  $VO_2$  at each speed (m/min) in KO and WT mice at 12 M. The simple linear function for KO (lower) and WT (upper) are shown. The slopes between the two regression lines were not significantly different at 21M. **Figure 1B:** Maximal work performed by KO and WT mice with age. WT slightly decrease the work performed ( $p=ns$ ) but the work performed by KO significantly decreased from  $17\pm 1.4$  mkg at 12M to  $9.4\pm 1.7$  mkg at 21M ( $p<0.001$ ). The simple linear regressions for KO and WT are shown. The slopes between the two regression lines were significantly different ( $p<0.01$ ). Values are mean  $\pm$  SEM.

**Figure 2A:** Maximal running distance by KO and WT mice with age. KO ran 20-60% less distance than WT at each age ( $p<0.001$ ). \*  $P<0.05$ : KO vs. WT at different ages. Values are mean  $\pm$  SEM. **Figure 2B:**  $VO_{2max}$  in KO and WT mice with age. The  $VO_{2max}$  of KO normalized to per work unit was significantly higher values starting from 14M to 21M compared to WT ( $p<0.05$ ). \*  $P<0.05$ : KO vs. WT at different age. Values are mean  $\pm$  SEM.

**Figure 3A:**  $VCO_{2max}$  in KO and WT mice with age. The  $VCO_{2max}$  of KO normalized to per work unit was significantly higher from 14M to 21M compared to WT ( $p<0.05$ ). \*  $P<0.05$ : KO vs. WT at different age. Values are mean  $\pm$  SEM. **Figure 3B:** RERmax in KO and WT mice with age. The RERmax of KO normalized to per work unit was

significantly higher compared to WT ( $p < 0.05$ ). \*  $P < 0.05$ : KO vs. WT at different age.

Values are mean  $\pm$  SEM.

**Figure 4A:** A Scatter plot of one of the KO mice versus the baseline which is the average of all the WT samples. The X-axis indicates the basal level of gene expression in WT controls and the Y-axis indicates the expression ratios comparing KO sample and baseline. Crosses shown in red and green represent genes which are up and downregulated in KO samples as compared to the baseline, respectively. **Figure 4B:** Percent of known genes in each functional category that are up and downregulated in KO mice. The percent upregulated is indicated above the line (Grey bars), and the percent downregulated is displayed below the line as negative values (Black bars).

**Supplementary Table 1:** Genes with increased and decreased expression in eNOS KO male mice.

### VO<sub>2</sub> at Each Speed in eNOS KO and WT Mice at 12M

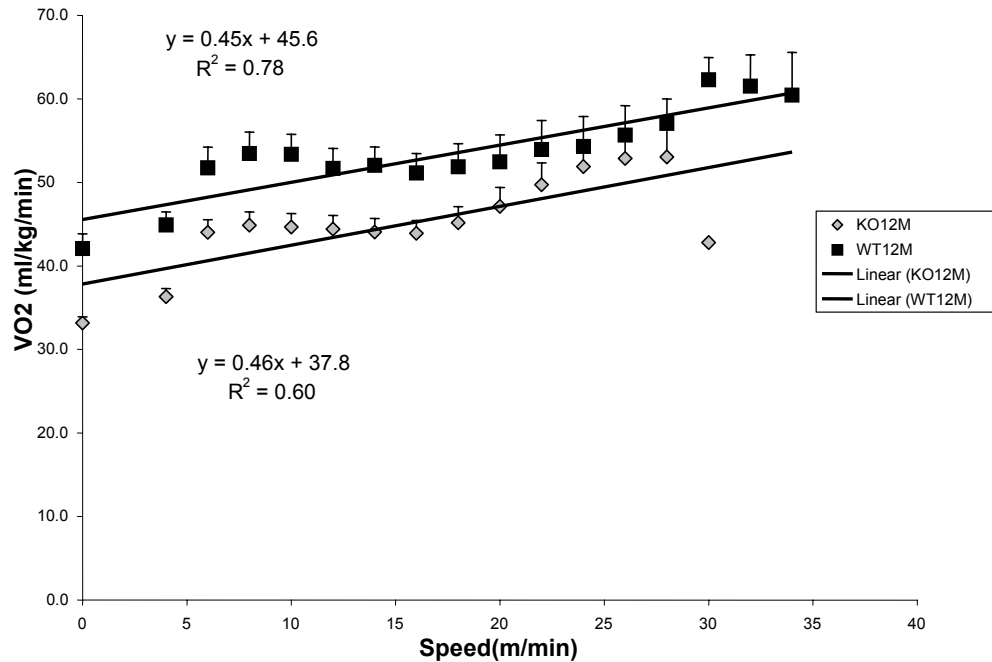


Figure 1A

### Work Performed with Age in eNOS KO and WT Mice

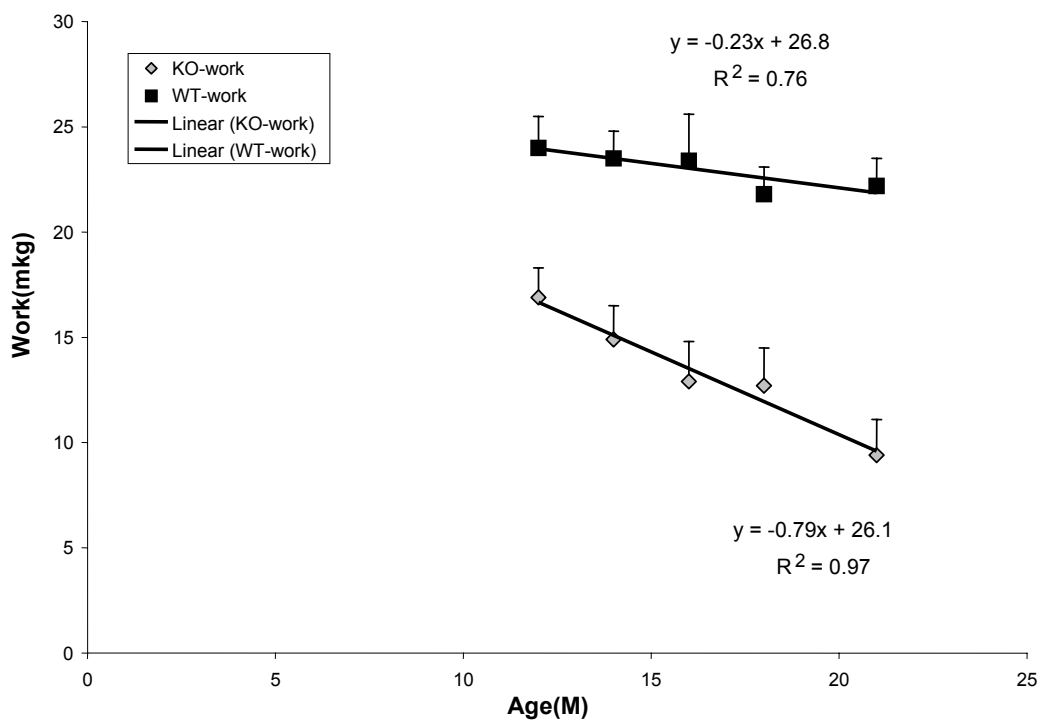


Figure 1B

### Running Distance in eNOS KO and WT Mice at Different Age

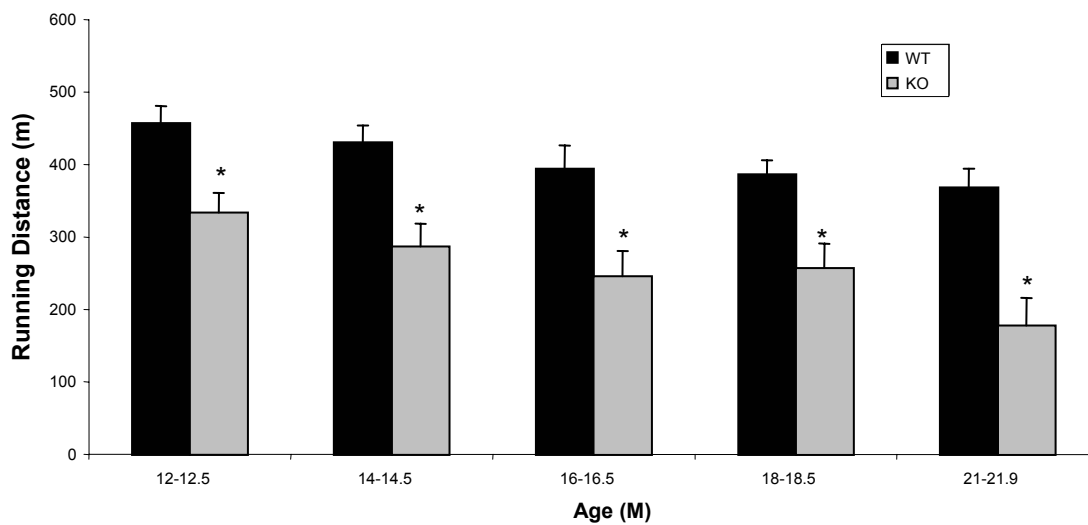


Figure 2A

### VO<sub>2</sub>max Per Work Unit in eNOS KO and WT Mice with Age

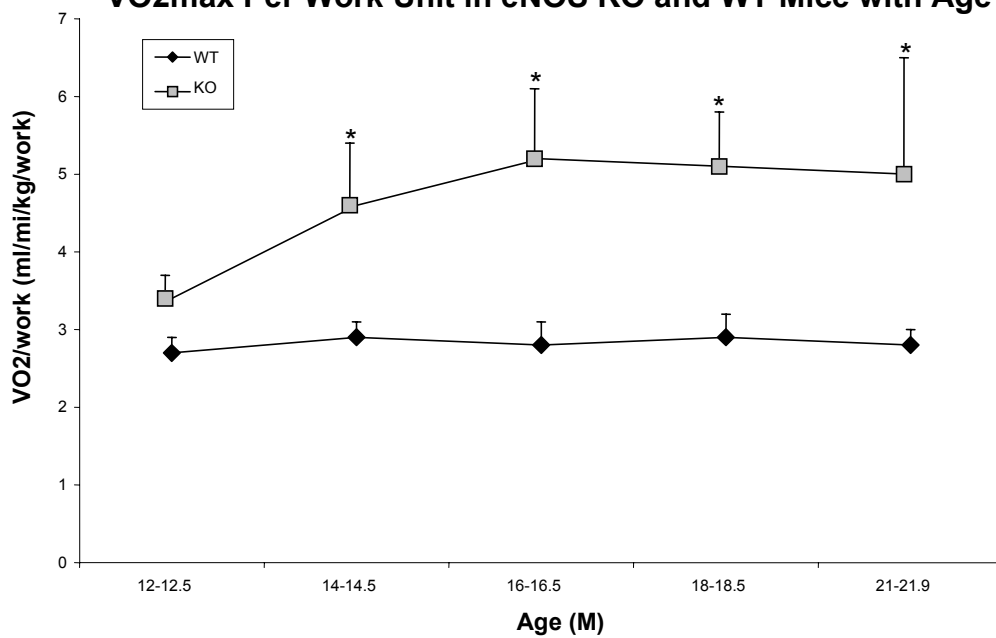


Figure 2B

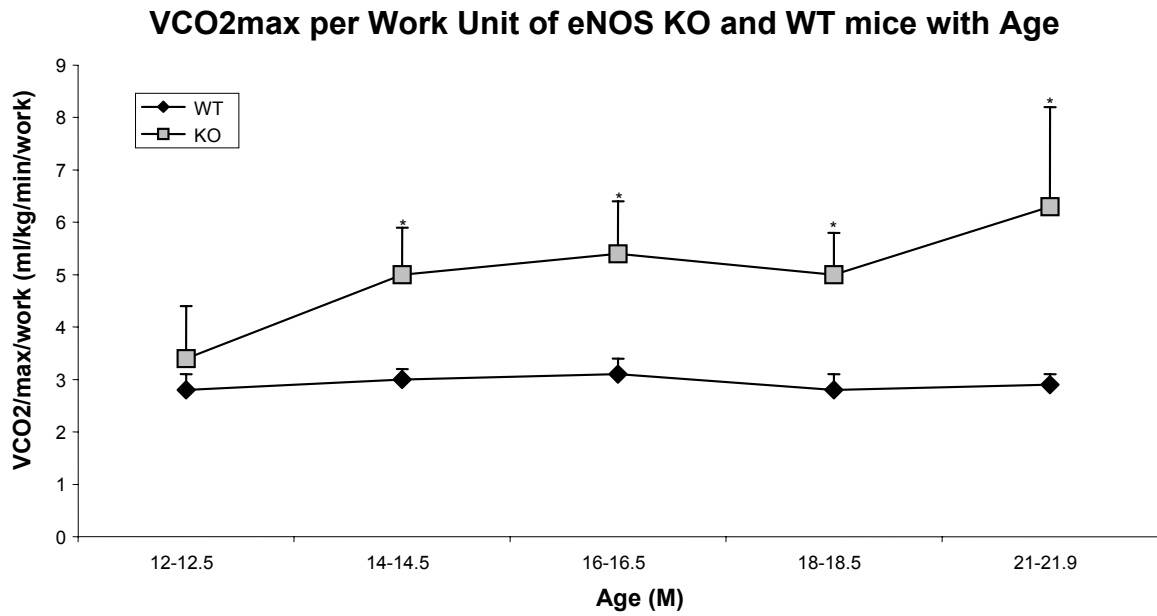


Figure 3A

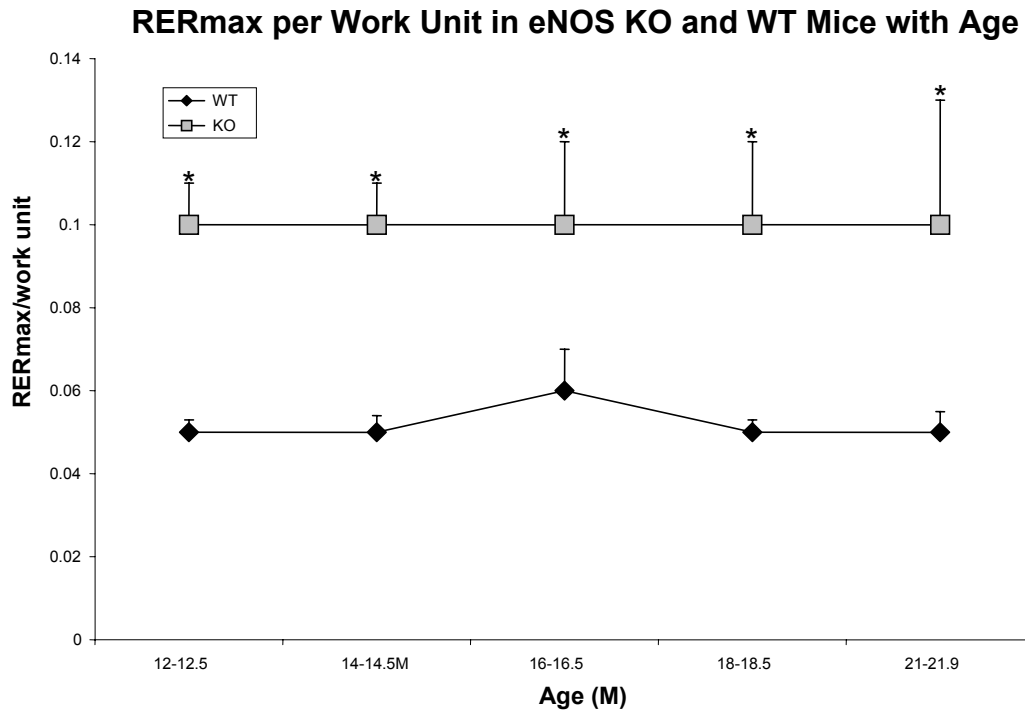


Figure 3B

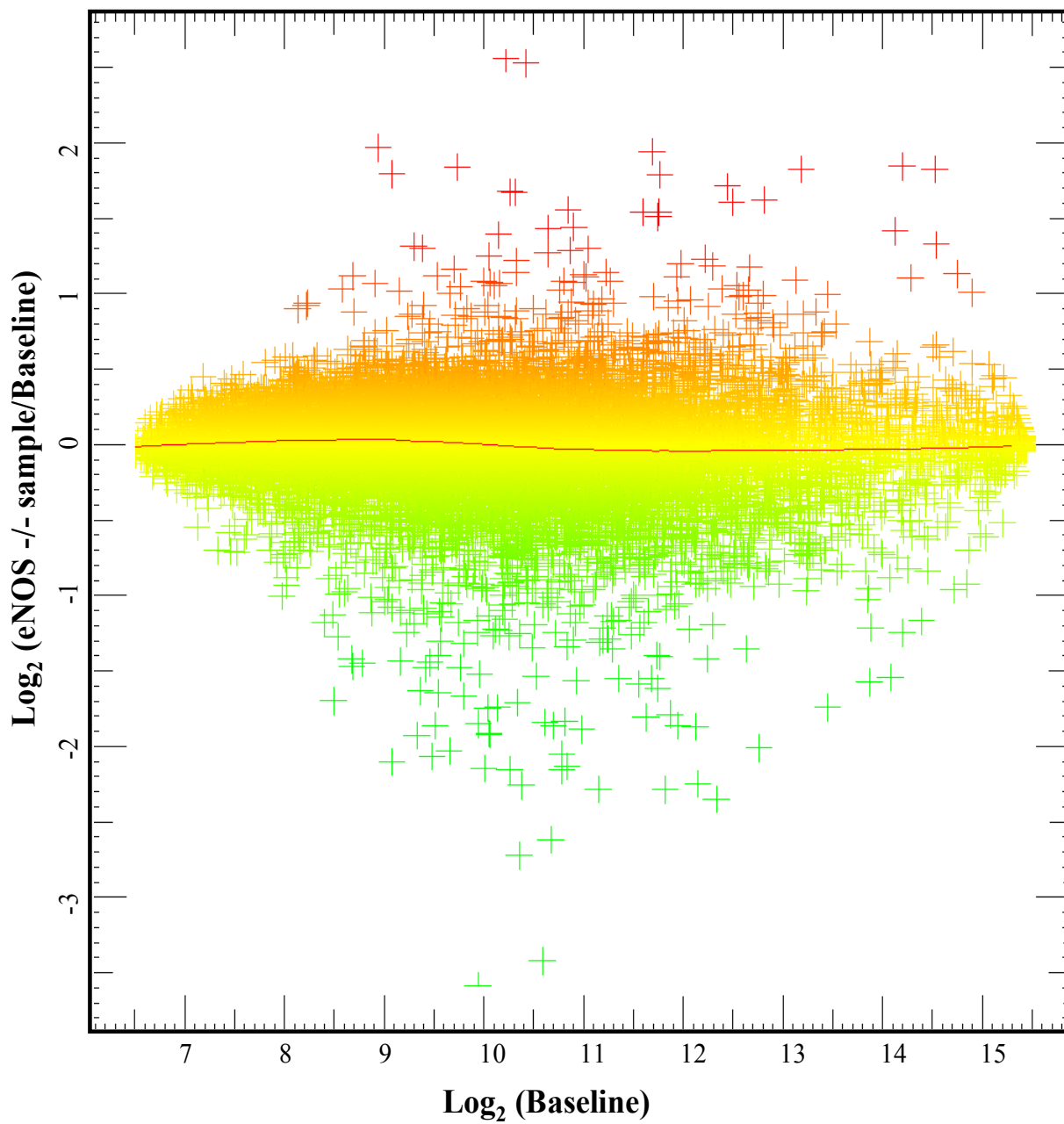


Figure 4A

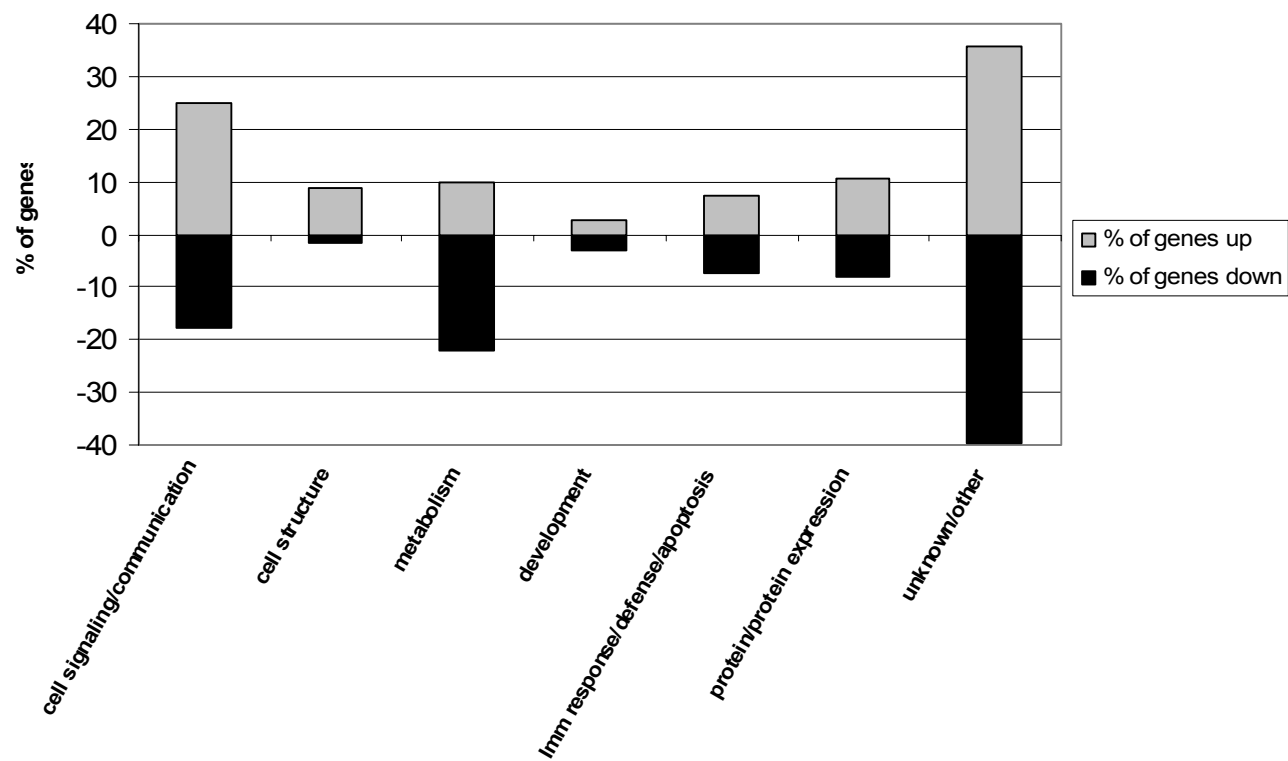


Figure 4B